




Article

Enhanced Tunability of $\text{BaTi}_x\text{Sn}_{1-x}\text{O}_3$ Films on Dielectric Substrate

Andrey Tumarkin ^{1,*}, Evgeny Sapego ¹, Alexander Gagarin ¹ and Stanislav Senkevich ²

¹ Faculty of Electronics, Saint Petersburg Electrotechnical University "LETI", Professora Popova Str. 5, 197376 Saint Petersburg, Russia; eugenysapego@yandex.ru (E.S.); aggagarin@gmail.com (A.G.)

² Division of Physics of Dielectrics and Semiconductors, Ioffe Institute, Polytechnicheskaja Str. 26, 194021 Saint Petersburg, Russia; senkevichsv@mail.ioffe.ru

* Correspondence: AVTumarkin@yandex.ru

Abstract: The structural properties of ferroelectric films of barium titanate-stannate on alumina substrates and the microwave characteristics of planar capacitive elements based on them are studied. It is established that the composition of the gas medium and the temperature of the substrate during the deposition of the film has a significant effect on the crystal structure, phase composition of the films and their electrical characteristics. Planar capacitors based on films subjected to high-temperature annealing after deposition exhibit 85% tunability at a frequency of 2 GHz, which is the best result for today.

Keywords: ferroelectrics; microwave properties; barium titanate-stannate; electrical tunable dielectric; XRD; Q-factor



Citation: Tumarkin, A.; Sapego, E.; Gagarin, A.; Senkevich, S. Enhanced Tunability of $\text{BaTi}_x\text{Sn}_{1-x}\text{O}_3$ Films on Dielectric Substrate. *Appl. Sci.* **2021**, *11*, 7367. <https://doi.org/10.3390/app11167367>

Academic Editor: Valentina Belova

Received: 18 July 2021

Accepted: 9 August 2021

Published: 10 August 2021

Publisher's Note: MDPI stays neutral with regard to jurisdictional claims in published maps and institutional affiliations.



Copyright: © 2021 by the authors. Licensee MDPI, Basel, Switzerland. This article is an open access article distributed under the terms and conditions of the Creative Commons Attribution (CC BY) license (<https://creativecommons.org/licenses/by/4.0/>).

1. Introduction

Ferroelectric thin-film materials (FE) demonstrate high nonlinearity of dielectric properties (the dependence of the permittivity on the strength of the applied electric field), which makes them promising materials for electrically tunable devices of microwave electronics. The advantages of ferroelectrics at microwaves are: high dielectric nonlinearity, relatively low losses, short switching time ($\sim 10^{-11}$ s), high operating power with low energy consumption in control circuits and high radiation resistance [1–10].

Among the ferroelectrics studied today, the most attractive for use at microwaves are perovskite oxide materials, which are capable of forming multicomponent solid solutions whose electrophysical properties can be changed in broad limits [11–14]. The most studied ferroelectric material for microwave applications is barium-strontium titanate $\text{Ba}_x\text{Sr}_{1-x}\text{TiO}_3$ (BST) [3–5], in which the formation of a solid solution occurs due to the substitution of A-site atom in ABO_3 perovskite structure. At the same time, there are a number of ferroelectrics, in which the formation of a solid solution occurs due to the B-site substitution [15,16]. Among them the barium titanate-stannate $\text{BaTi}_x\text{Sn}_{1-x}\text{O}_3$ (BTS) is a potentially promising material for electrically tunable applications. Depending on the ratio of the concentrations of Ti and Sn atoms, the value of the relative dielectric permittivity of BTS solid solution in the maximum can reach significant values $(2-3) \times 10^4$ [15]; the introduction of chemically more stable Sn atoms into a solid solution instead of Ti can lead to a decrease in through conductivity and dielectric losses, to a significant increase in the electrical strength of the material, and, as a result, to the possibility of increasing the applied electric field and increasing the dielectric nonlinearity [16]. A number of papers have been published that investigate the structural and electrophysical properties of BTS thin films [15–34], including works dedicated to microwave investigations [25,34,35]. The studied films were obtained by chemical solution deposition [22,23,36], ion-plasma sputtering [17–19,29,30,34,35], sol-gel technology [24–28,31,32] and laser ablation [33]. In the vast majority of works, experimental data on dielectric losses in FE capacitive structures are given for the frequency range of

1 kHz–1 MHz. These data do not allow us to draw a conclusion about the applicability of the obtained films at microwaves.

In addition, it should be noted that the high dielectric nonlinearity of capacitive elements based on the studied films (tunability up to 72%) is demonstrated exclusively in plane-parallel metal-dielectric-metal (MDM) structures, i.e., in cases when the film is formed on a conducting electrode [22–24,28–30,33,35], while in works devoted to the growth of FE layers on dielectric materials data on tunability from 15 to 46% are given [25–27,31,32,34,36], and only on expensive monocrystal substrates. The design of MDM capacitors allows the use of small control voltages to change the capacitance, but exactly because of it, the use of such structures is possible only in small-signal devices. However, one of the main potential advantages of FE devices over semiconductor analogues, namely the ability to operate at high power levels, can only be realized in a planar design on a dielectric substrate.

Therefore, more investigations are necessary in order to obtain enhanced tunability of BTS thin films on dielectric substrates with high Q-factor and low cost.

As one such substrate material, polycrystalline aluminum oxide can be proposed. Alumina has excellent mechanical and dielectric properties: surface roughness of about 0.05 μm , thermal coefficient of linear expansion 8×10^{-6} , which is close to BTS one, high thermal conductivity coefficient of about 30 W/m \times K, stable dielectric permittivity 9.7, low losses at microwaves ($\tan \delta < 10^{-4}$), and extremely low cost.

In this regard, the purpose of this work is to search for technological approaches that allow to obtain thin layers of barium titanate-stannate, showing high nonlinearity, on alumina substrate, to study the structure and high-frequency dielectric properties of thin BTS layers grown at various temperatures, with the aim of their further application as part of high-power microwave nonlinear elements.

2. Materials and Methods

The deposition of coatings was carried out by RF magnetron sputtering of a ceramic target of the composition $\text{BaTi}_{0.8}\text{Sn}_{0.2}\text{O}_3$ on alumina substrates (polycrystalline aluminum oxide Al_2O_3). The temperature of the substrate T_s was varied in the range of 650–850 $^\circ\text{C}$. A mixture of Ar/ O_2 was used as the working gas, the oxygen content in the mixture was varied from 0 to 40%. The working gas pressure was 2 Pa. The thickness of the films was 400 nm and 800 nm. After deposition, the films were annealed at a temperature of 1100 $^\circ\text{C}$ in air for 2 h.

The crystal structure and phase composition of the films were studied by X-ray diffraction using a DRON-6 diffractometer on the CuK α 1 emission spectral line ($\lambda = 1.5406 \text{ \AA}$). The parameters of the crystal lattice of BTS films were calculated based on the angular positions of X-ray reflexes, using reflections from the substrate as a reference. The surface morphology was studied by atomic force microscopy (AFM) on a scanning probe microscope Solver-P47Pro from NT-MDT in a semi-contact mode. The scanning resolution was 512×512 pixels. Cantilevers of the NSG01 type with an average resonant frequency of 150 kHz and an average radius of curvature of the tip of 6 nm were used. Before the measurements the device was calibrated using NT-MDT TGS1 test grids.

For electrical research, planar capacitors were formed on the basis of BTS films. The upper electrodes of the capacitors were made by thermal evaporation of a Cu film (1 μm) with an adhesive chromium sublayer, followed by lithography and chemical etching. The capacitance C - and Q-factor $Q = 1/\tan \delta$ of the capacitors were measured at a frequency of 2 GHz using a half-wave strip resonator [37] and HP 8719C vector analyzer. The resonator provides an unloaded Q-factor of 1000 (the accuracy of measuring the capacitance and Q-factor is 1 and 5%, respectively), as well as the possibility of supplying a control voltage up to 1000 V. The tunability of the capacitors was calculated as the ratio of capacitances at zero and maximum applied control voltage $n = C(0 \text{ V})/C(U_{\text{max}})$, and additionally as $n = (C_{\text{max}} - C_{\text{min}})/C_{\text{max}}$ in order to compare results with other works.

3. Results

The electrical characteristics of multicomponent films are determined by the crystal structure of the material, the component and phase composition, the size of the crystallites, the presence of impurity phases and deformations of the crystal lattice. These factors significantly affect the dielectric permittivity of FE films, as well as the nonlinearity, losses and performance of devices based on them. For the development of ferroelectric microwave devices, it is important to understand the relationship between the structural and electrical properties of films and the technological conditions of their formation.

The results of recent studies indicate a significantly different effect of the composition of the gas medium in which the formation of FE film occurs on their structural properties and phase composition. Thus, the perovskite crystal structure of barium-strontium titanate without secondary phases is confidently formed in a purely oxygen medium on sapphire, silicon carbide, magnesium oxide, etc. On the other hand, it is noted in [34,38] that attempts to form FE film with substitution of Ti by Zr or Sn atoms on dielectric substrates in an oxygen-rich gas medium lead to the formation of a multiphase structure consisting of purely dielectric barium zirconates or barium stannates and secondary phases with a high content of titanium—simple oxides and barium polytitanates (BaTi_2O_5 , $\text{BaTi}_5\text{O}_{11}$, etc.). This can be explained by the kinetics of Ti oxidation in a medium with a high oxygen content, when the rate of formation of secondary phases of titanium significantly exceeds the rate of formation of ferroelectric BaTiO_3 . In this case, the absence of free Ti on the substrate surface may cause the formation of pure barium zirconates/stannates. The situation is complicated by the fact that many titanates have a similar crystal structure [39–41], which often leads to the overlap of diffraction reflections from different phases and complicates their identification. Each of these compounds has its own permittivity ϵ and the dependence $\epsilon(T)$, which can affect the electrophysical properties of the ferroelectric device as a whole. It follows that for the formation of single-phase films of barium titanate-stannate on dielectric substrates by deposition from the gas phase, the oxygen content in the working gas should not exceed 50%.

Figure 1 shows the diffractograms of BTS films deposited on alumina at a substrate temperature of $T_s = 650^\circ\text{C}$ and at different concentrations of oxygen in the working gas. At the angles 32° , 39° , 45° , 55° , the dotted lines on the left correspond to the positions of the reflexes for pure barium stannate, the lines on the right correspond to the barium titanate, the reflexes from the substrate are marked with diamonds (PDF 46-1212). Three factors draw attention to themselves. (i) In pure argon, the structure of perovskite is practically not formed. (ii) For films deposited in a medium containing 40% oxygen in a gas mixture, the positions of the reflexes correspond to BaSnO_3 with the lattice parameter 4.12 \AA , without signs of the presence of a solid solution. The probable cause of the formation of the dielectric barium stannate may be the presence of impurity phases of titanium oxides on the substrate, the possible positions of XRD reflexes from which are marked in Figure 1 with red and blue dotted lines (PDF 21-1272 TiO_2 Anatase; PDF 8-117 TiO; PDF 29-1360 TiO_2 Brookite; PDF 34-133 BaTi_2O_5), similar to [34,38]. (iii) The reflexes from the BTS phase in Figure 1 are significantly shifted towards large angles when the oxygen content in the gas medium decreases from 40 to 20%, that for polycrystalline samples means a change in the composition of the solid solution (the ratio of Ti and Sn) according to the Vegard's law (see the inset in Figure 1) [42]. The deposition of the BTS film in a gas medium containing 20% oxygen leads to the formation of (211) textured coating with the lattice parameter 4.09 \AA , which corresponds to the composition $\text{BaTi}_{0.28}\text{Sn}_{0.72}\text{O}_3$ solid solution.

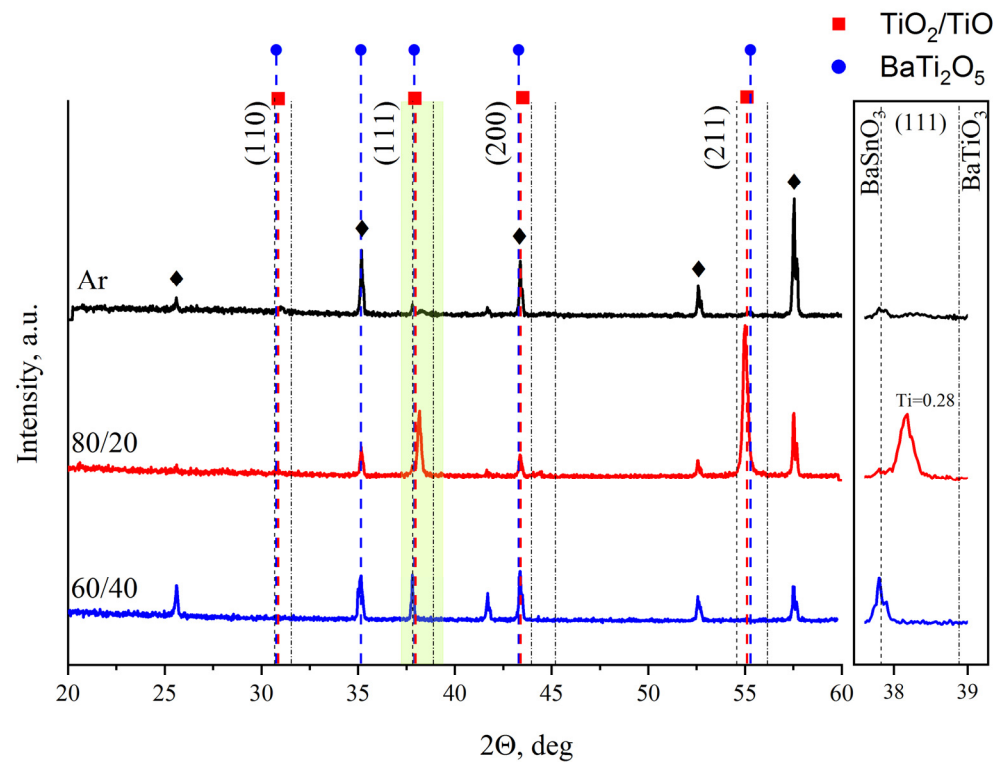


Figure 1. Diffractograms of the BTS thin films on Al_2O_3 substrates deposited at different oxygen concentrations in gas ambient.

Figure 2 demonstrates diffractograms of BTS films deposited on alumina in the substrate temperature range of $T_s = 650\text{--}850\text{ }^\circ\text{C}$ in a gas mixture of Ar (80%)/ O_2 (20%). The dotted lines correspond to the positions of the reflexes for $\text{BaTi}_{0.8}\text{Sn}_{0.2}\text{O}_3$ sputtered target. It is seen that an increase in the deposition temperature leads to a change in the growth texture from (211) to (110), as well as to a shift of reflexes towards large angles, which indicates a decrease in the lattice parameter of films from 4.09 \AA till 4.07 \AA , and, hence, an increase in the concentration of barium titanate in a solid solution from 28% ($\text{BaTi}_{0.28}\text{Sn}_{0.72}\text{O}_3$) to 40% ($\text{BaTi}_{0.4}\text{Sn}_{0.6}\text{O}_3$), and an approach of the component composition of the film to the composition of the sputtered target (see the inset in Figure 2). At a temperature of $850\text{ }^\circ\text{C}$, the film solid solution reveals the pronounced preferential orientation (110). However, despite the positive trend of increasing the content of BaTiO_3 in solid solution with increasing T_s , stoichiometric transfer of the target composition into the film by increasing the deposition temperature cannot be achieved. It can be assumed that secondary phases rich in titanium are still present in the films, the content of which decreases with an increase in the deposition temperature.

Figure 3 shows the diffractograms of the above-described BTS films but subjected to high-temperature annealing in air at a temperature of $1100\text{ }^\circ\text{C}$ for two hours. Post-growth high-temperature treatment radically changes the structural properties of the studied films. During annealing, titanium is redistributed between the secondary phases and the main phase of BTS, as a result of which the composition of the film solid solution after annealing repeats the composition of the $\text{BaSn}_{0.2}\text{Ti}_{0.8}\text{O}_3$ target with the lattice parameter 4.03 \AA (see inset with reflex (211) in Figure 3). In addition, for films deposited at $T_s = 650$ and $700\text{ }^\circ\text{C}$, annealing leads to an increase in the intensity of the reflex (111), and for films grown at $T_s = 800$ and $850\text{ }^\circ\text{C}$, to a decrease in the width of the dominant reflex (110), which indicates an improvement in the quality of the crystal lattice of the coatings under study.

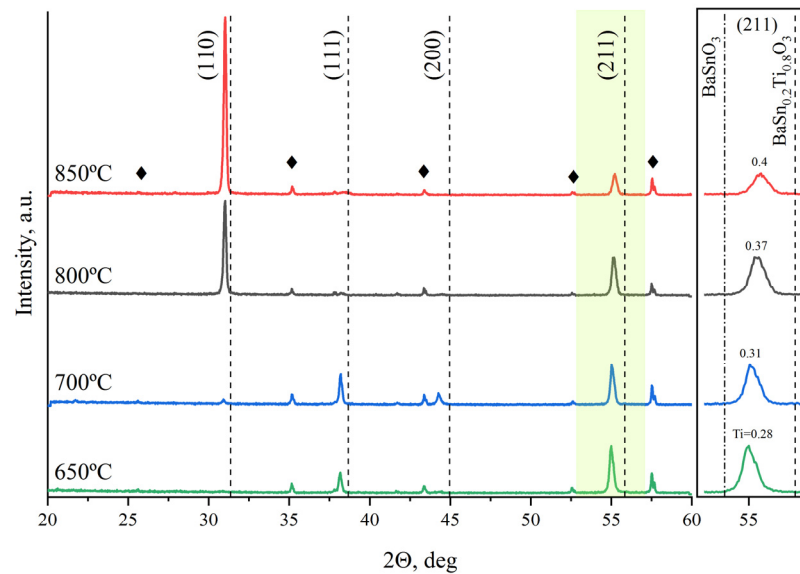


Figure 2. Diffractograms of the BTS thin films on Al_2O_3 substrates at different substrate temperatures.

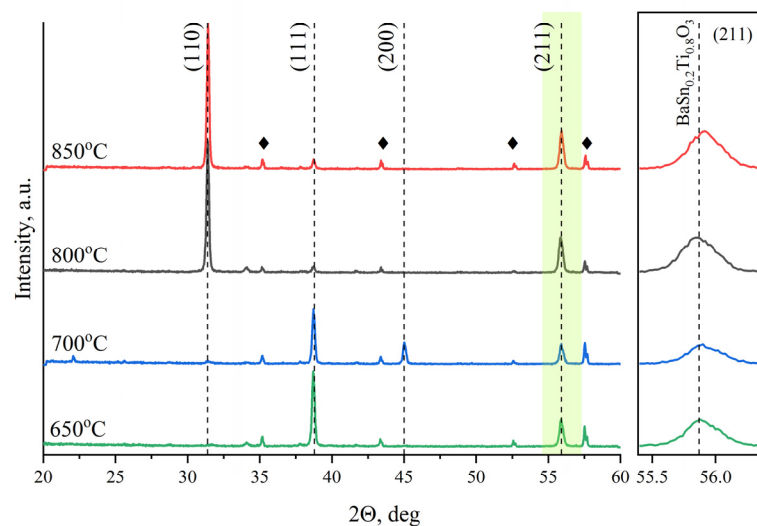


Figure 3. Diffractograms of the BTS thin films on Al_2O_3 substrates at different substrate temperatures after annealing at 1100°C in air.

Figure 4 shows the AFM images of the surface of the studied samples before and after annealing. The linear substrate defects typical for polycrystalline aluminum oxide are clearly visible in the image before annealing, indicating that the film repeats the morphology of the substrate. The grains dimension of the non-annealed sample is about 150–300 nm (Figure 4a) and the surface roughness is about 20–30 nm (Figure 4b). According to the Figure 4c, as a result of annealing, the structure of the film surface becomes finer grained, the grain dimensions decrease to 50–150 nm, the grain boundaries become more pronounced, and the surface roughness decreases to 10–15 nm (Figure 4d).

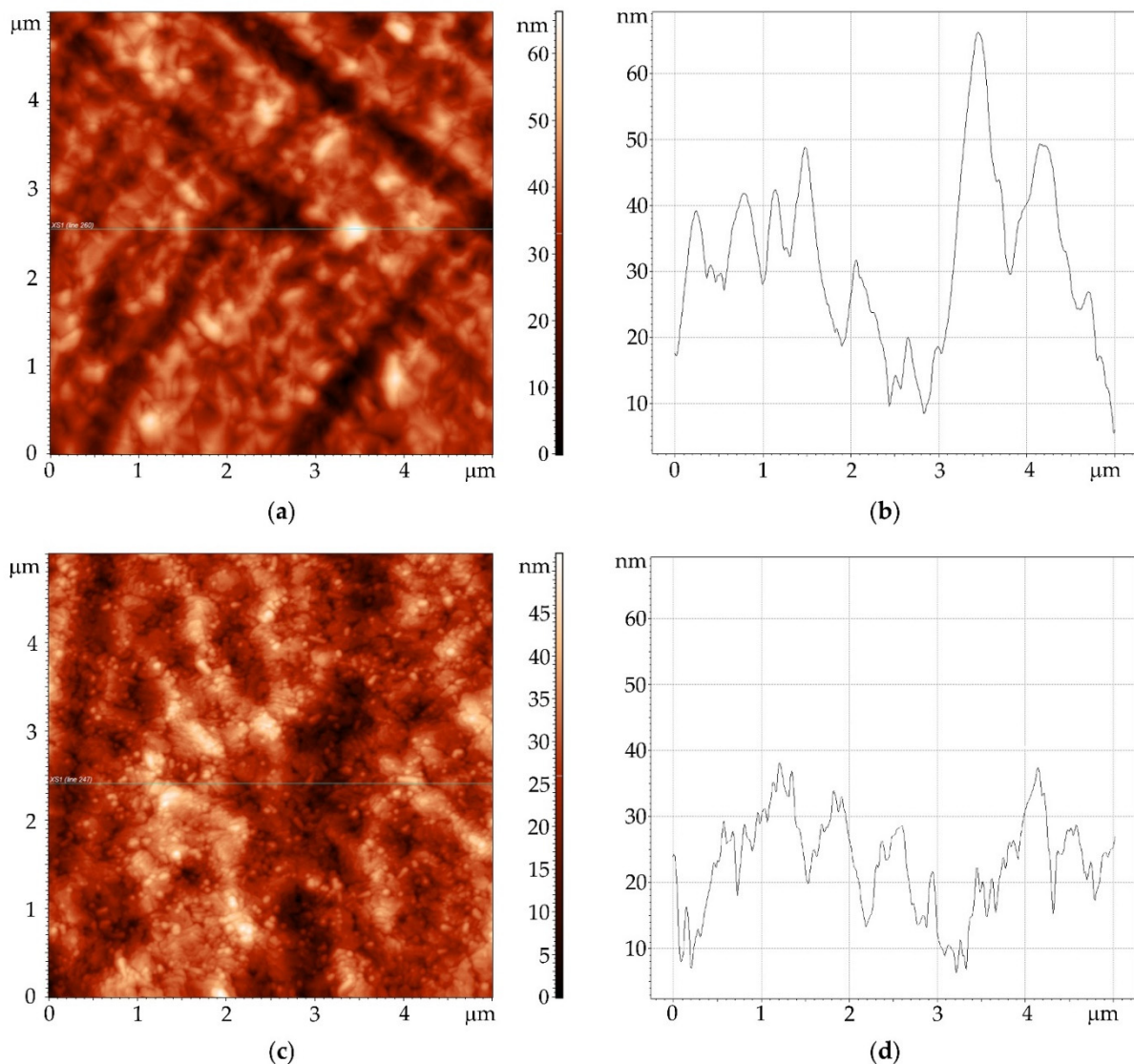


Figure 4. ACM images of BTS films on alumina before (a,b) and after (c,d) annealing.

Planar capacitors are formed on the basis of BTS films deposited in a gas medium Ar(80%)/O₂(20%) at different substrate temperatures. The dependences of the capacitance normalized by the maximum value of the capacitors under study on the strength of the control electric field are shown in Figure 5. It follows from the figure that the capacitor based on the non-annealed film exhibits minimal tunability, which is explained by the composition of the solid solution BaTi_{0.4}Sn_{0.6}O₃, most of which is a linear dielectric BaSnO₃. The tunability of capacitors formed on the basis of annealed films of BaTi_{0.8}Sn_{0.2}O₃ composition depends on film thickness. For films of 400 nm thickness, it increases from 2.8 to 3.4 with an increase in the deposition temperature from 650 to 850 °C. The tunability of capacitor based on 800 nm film is 6.8 times (85%), which is the best result for BTS capacitors today. For a capacitor with a planar structure, the total capacitance is composed of three components: air, BTS film and substrate. In this configuration, tunability only comes from BTS film since the substrate shows no tunability, being the linear dielectric. Then the thickness of the FE film will affect the tunability, because in the case of a thin FE film, some part of the field will penetrate into the substrate with a low dielectric constant.

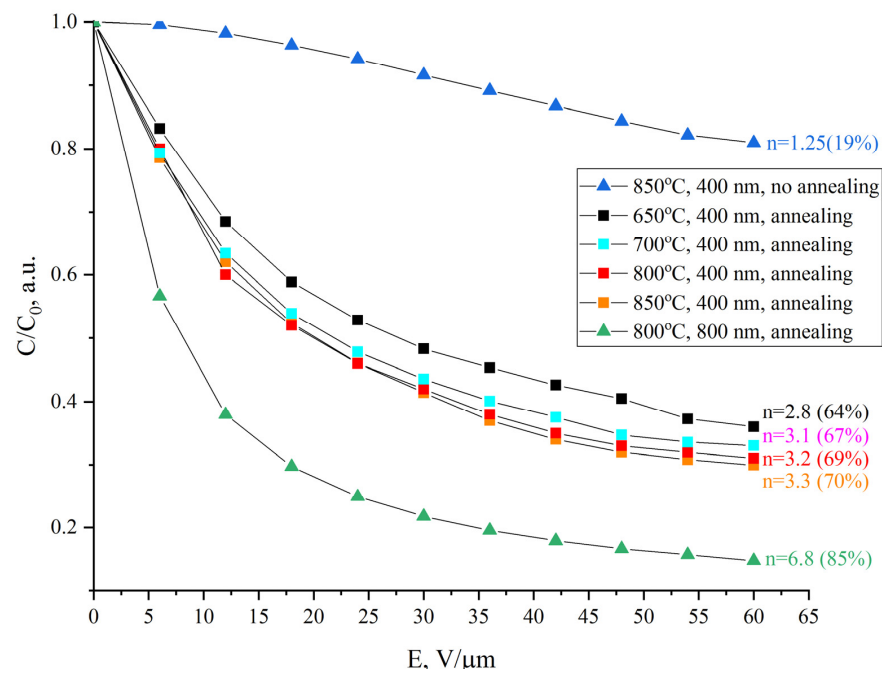


Figure 5. Dependencies of the capacitances of the BTS films based planar capacitors on control electric field strength.

The dependences of the Q-factor of the same capacitive structures on the strength of the control field, measured at a frequency of 2 GHz, are shown in Figure 6. Three groups of curves can be distinguished here. (1) The relatively high Q-factor of a capacitor based on a non-annealed film is explained by 60% of barium stannate in a solid solution. (2) The Q-factor of capacitors based on films deposited at a temperature of 800 °C and above increases from 10 to 55–60 under the action of an applied field, which can be explained by their well-formed predominantly oriented crystal structure (see Figure 3). (3) The low Q-factor of capacitors based on films formed at substrate temperatures of 650–700 °C is due to the polycrystalline structure of these films when the grain boundaries make an additional contribution to the dielectric losses of the capacitor.

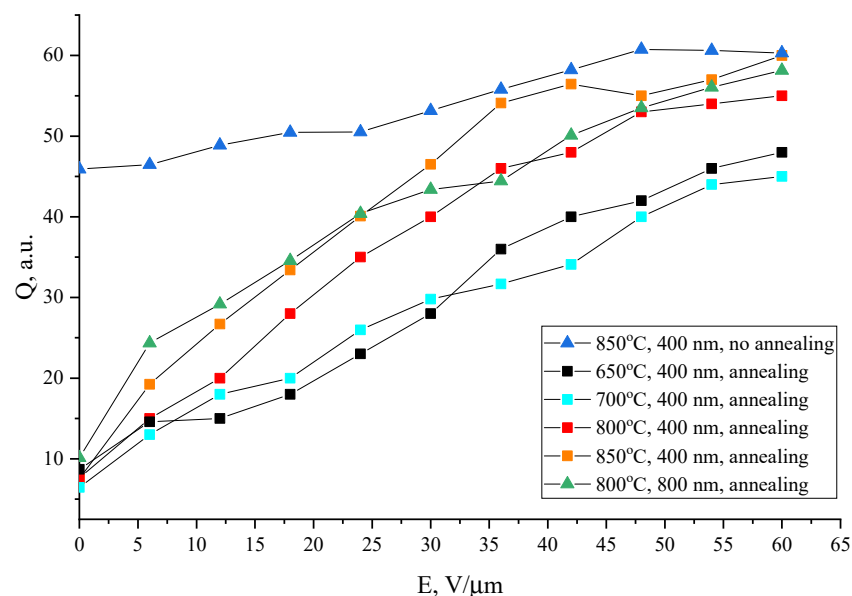


Figure 6. Dependencies of the Q-factor of the BTS based planar capacitors on control electric field strength.

4. Discussion

Table 1 presents comparative data on the tunability of MDM and planar capacitors based on barium titanate-stannate films. It follows from the table data that the capacitors obtained in this work exhibit high dielectric nonlinearity in the microwave range, which is the best result published today for both sandwich and planar capacitive structures based on BTS films. Three factors can determine such a high tunability: the predominantly oriented crystal lattice of the sample deposited at a substrate temperature of more than 800 °C; the component composition of a solid solution with a high content of nonlinear barium titanate, obtained as a result of annealing; the absence of impurity phases of linear dielectrics in the high tunability sample. These results indicate an attractive prospect for electrically tunable applications of BTS capacitive structures in microwave electronics.

Table 1. Data on the tunability of MDM and planar capacitors based on barium titanate-stannate films.

Composition	Substrate	Construction	Tunability, %	Reference
BaTi _{0.85} Sn _{0.15} O ₃	Pt/Si	MDM	66	[15]
BaTi _{0.85} Sn _{0.15} O ₃	Pt/Si	MDM	65	[16]
BaTi _{0.75} Sn _{0.25} O ₃	Cu	MDM	50	[20]
BaTi _{0.85} Sn _{0.15} O ₃	LaNiO ₃ /LaAlO ₃	MDM	68	[24]
BaTi _{0.85} Sn _{0.15} O ₃	LaNiO ₃ /LaAlO ₃	MDM	43	[22]
BaTi _{0.85} Sn _{0.15} O ₃	LaNiO ₃ /SrTiO ₃	MDM	45	[22]
BaTi _{0.85} Sn _{0.15} O ₃	LaNiO ₃ /MgO	MDM	50	[22]
BaTi _{0.85} Sn _{0.15} O ₃	LaNiO ₃ /Al ₂ O ₃	MDM	57	[22]
BaTi _{0.85} Sn _{0.15} O ₃	LaNiO ₃ /Si	MDM	54	[26]
BaTi _{0.85} Sn _{0.15} O ₃	ITO/glass	MDM	58	[17]
BaTi _{0.85} Sn _{0.15} O ₃	Pt/Si	MDM	72	[18]
BaTi _{0.85} Sn _{0.15} O ₃	Cu	MDM	67	[19]
BaTi _{0.85} Sn _{0.15} O ₃	LaAlO ₃	planar	17	[23]
BaTi _{0.85} Sn _{0.15} O ₃	MgO	planar	15	[29]
BaTi _{0.85} Sn _{0.15} O ₃	Sapphire	planar	20	[25]
BaTi _{0.85} Sn _{0.15} O ₃	LaAlO ₃	planar	46	[34]
BaTi _{0.85} Sn _{0.15} O ₃	SrTiO ₃	planar	46	[30]
BaTi _{0.8} Sn _{0.2} O ₃	Alumina	planar	85	This work

5. Conclusions

The results of the conducted studies have shown that when BTS films are deposited on dielectric substrate in a gas medium with an oxygen content of 40% or more, the main phase formed on the substrate is pure barium stannate, with the probable presence of secondary titanium oxides, which determines the absence of nonlinear dielectric properties of these films. The films deposited in the gas mixture Ar/O₂ 80/20 are a solid solution of BaTi_xSn_{1-x}O₃ with a composition and growth orientation depending on the deposition temperature. BTS films subjected to high-temperature annealing in air have a well-formed crystal lattice at the absence of secondary phase inclusions, their component composition repeats the composition of the target, which has a positive effect on their electrophysical properties, in particular on the nonlinearity and the level of dielectric losses. A comparison of the results obtained with the literature data showed that planar BTS structures on alumina exhibit promising characteristics for an elaboration of high-power microwave tunable devices based on them.

Author Contributions: Conceptualization, A.T.; methodology, A.T., A.G.; software, E.S.; validation, A.T., A.G.; formal analysis, E.S., A.G., S.S.; investigation, E.S., A.G., S.S.; resources, A.T.; writing—original draft preparation, A.T.; writing—review and editing, A.T.; visualization, E.S., S.S.; supervision, A.T.; project administration, A.T.; funding acquisition, A.T. All authors have read and agreed to the published version of the manuscript.

Funding: This research was funded by Russian Foundation for Basic Research (RFBR), grant number 19-37-90055.

Institutional Review Board Statement: Not applicable.

Informed Consent Statement: Not applicable.

Data Availability Statement: Not applicable.

Conflicts of Interest: The authors declare no conflict of interest.

References

1. Aspe, B.; Cissé, F.; Castel, X.; Demange, V.; Députier, S.; Ollivier, S.; Guilloux-Viry, M. $K_xNa_{1-x}NbO_3$ perovskite thin films grown by pulsed laser deposition on R-plane sapphire for tunable microwave devices. *J. Mater. Sci.* **2018**, *53*, 13042–13052. [[CrossRef](#)]
2. Aldrigo, M.; Dragoman, M.; Laudadio, E.; Iordanescu, S.; Modreanu, M.; Povey, I.M.; Mencarelli, D. Microwave applications of zirconium-doped hafnium oxide ferroelectrics: From nanoscale calculations up to experimental results. In Proceedings of the 2020 IEEE/MTT-S International Microwave Symposium (IMS), Los Angeles, CA, USA, 4–6 August 2020; pp. 520–523.
3. Crunteanu, A.; Muzzupapa, V.; Ghalem, A.; Huitema, L.; Passerieux, D.; Borderon, C.; Gundel, H.W. Characterization and Performance Analysis of BST-Based Ferroelectric Varactors in the Millimeter-Wave Domain. *Crystals* **2021**, *11*, 277. [[CrossRef](#)]
4. Parsa, N.; Gasper, M.R.; Toonen, R.C.; Ivill, M.P.; Hirsch, S.G. Microwave power detection using ferroelectric thin film varactors. *Integr. Ferroelectr.* **2018**, *192*, 1–9. [[CrossRef](#)]
5. Aymen, S.; Mascot, M.; Jomni, F.; Carru, J.C. High tunability in lead-free $Ba_{0.85}Sr_{0.15}TiO_3$ thick films for microwave tunable applications. *Ceram. Int.* **2019**, *45*, 23084–23088. [[CrossRef](#)]
6. Vendik, O.G.; Zubko, S.P. Ferroelectrics as Constituents of Tunable Metamaterials. In *Theory and Phenomena of Metamaterials*; CRC Press: Boca Raton, FL, USA, 2017; p. 33-1.
7. Martínez-Viviente, F.L.; Hinojosa, J. Tunable ferroelectrics for frequency agile microwave and THz devices. In *Magnetic, Ferroelectric, and Multiferroic Metal Oxides*; Elsevier: Amsterdam, The Netherlands, 2018; pp. 251–264.
8. Gupta, R.; Rana, L.; Sharma, A.; Freundorfer, A.P.; Sayer, M.; Tomar, M.; Gupta, V. High frequency coplanar microwave resonator using ferroelectric thin film for wireless communication applications. *Mater. Today Proc.* **2018**, *5*, 15395–15398. [[CrossRef](#)]
9. Pronin, I.P.; Kaptelov, E.Y.; Tarakanov, E.A.; Afanas'ev, V.P. Effect of annealing on the self-poled state in thin ferroelectric films. *Phys. Solid State* **2002**, *44*, 1736–1740. [[CrossRef](#)]
10. Firsova, N.Y.; Mishina, E.D.; Sigov, A.S.; Senkevich, S.V.; Pronin, I.P.; Kholkin, A.; Yuzyuk, Y.I. Femtosecond infrared laser annealing of PZT films on a metal substrate. *Ferroelectrics* **2012**, *433*, 164–169. [[CrossRef](#)]
11. Osipov, V.V.; Kiselev, D.A.; Kaptelov, E.Y.; Senkevich, S.V.; Pronin, I.P. Internal field and self-polarization in lead zirconate titanate thin films. *Phys. Solid State* **2015**, *57*, 1793–1799. [[CrossRef](#)]
12. Afanasjev, V.P.; Chigirev, D.A.; Mukhin, N.V.; Petrov, A.A. Formation and properties of PZT-PbO thin heterophase films. *Ferroelectrics* **2016**, *496*, 170–176. [[CrossRef](#)]
13. Oseev, A.; Lucklum, R.; Zubtsov, M.; Schmidt, M.P.; Mukhin, N.V.; Hirsch, S. SAW-based phononic crystal microfluidic sensor-microscale realization of velocimetry approaches for integrated analytical platform applications. *Sensors* **2017**, *17*, 2187. [[CrossRef](#)] [[PubMed](#)]
14. Afanasjev, V.P.; Mukhin, N.V.; Redka, D.N.; Rudenko, M.V.; Terukov, E.I.; Oseev, A.; Hirsch, S. Surface modification of ZnO by plasma and laser treatment. *Ferroelectrics* **2017**, *508*, 124–129. [[CrossRef](#)]
15. Zhao, C.; Huang, Y.; Wu, J. Multifunctional barium titanate ceramics via chemical modification tuning phase structure. *InfoMat* **2020**, *2*, 1163–1190. [[CrossRef](#)]
16. Huang, Y.; Zhao, C.; Zhong, S.; Wu, J. Highly Tunable Multifunctional $BaTiO_3$ -Based Ferroelectrics via Site Selective Doping Strategy. *Acta Mater.* **2021**, *209*, 116792. [[CrossRef](#)]
17. Wu, M.; Zhang, C.; Yu, S.; Li, L. Effect of sputtering pressure on structural and dielectric tunable properties of $BaSn_{0.15}Ti_{0.85}O_3$ thin films grown by magnetron sputtering. *Ceram. Int.* **2018**, *44*, 10236–10240. [[CrossRef](#)]
18. Wu, M.; Zhang, C.; Yu, S.; Li, L. Thickness dependence of microstructure, dielectric and leakage properties of $BaSn_{0.15}Ti_{0.85}O_3$ thin films. *Ceram. Int.* **2018**, *44*, 11466–11471. [[CrossRef](#)]
19. Zhu, G.S.; Xu, H.R.; Li, J.J.; Wang, P.; Zhang, X.Y.; Chen, Y.D.; Yu, A.B. Study on the influence of powder size on the properties of BTS/ITO thin film by RF sputtering from powder target. *Mater. Lett.* **2017**, *194*, 90–93. [[CrossRef](#)]
20. Chen, S.; Yu, S.; Zhang, B.; Zhang, J.; Ma, B.; Liu, Q.; Zhang, W. Pulsed laser deposition BTS thin films: The role of substrate temperature. *Ceram. Int.* **2016**, *42*, 9341–9346. [[CrossRef](#)]
21. Wu, M.; Li, X.; Dong, H.; Yu, S.; Li, L. High-performance flexible dielectric tunable BTS thin films prepared on copper foils. *Ceram. Int.* **2019**, *45*, 16270–16274. [[CrossRef](#)]
22. Ihlefeld, J.F.; Borland, W.J.; Maria, J.P. Synthesis and properties of barium titanate stannate thin films by chemical solution deposition. *J. Mater. Sci.* **2008**, *43*, 4264–4270. [[CrossRef](#)]
23. Yoon, K.H.; Park, J.H.; Jang, J.H. Solution deposition processing and electrical properties of $Ba(Ti_{1-x}Sn_x)O_3$ thin films. *J. Mater. Res.* **1999**, *14*, 2933–2939. [[CrossRef](#)]

24. Song, S.; Zhai, J.; Gao, L.; Yao, X. The effect of stress on the dielectric and tunable properties of barium stannate titanate thin films. *Appl. Phys. Lett.* **2009**, *94*, 052902. [[CrossRef](#)]
25. Song, S.N.; Zhai, J.W.; Yao, X. Dielectric and microwave properties of Ba (Sn_{0.15}Ti_{0.85})O₃ thin films. *Mater. Lett.* **2008**, *62*, 1173–1175. [[CrossRef](#)]
26. Gao, L.; Zhai, J.; Song, S.; Yao, X. Crystal orientation dependence of the out-of-plane dielectric properties for barium stannate titanate thin films. *Mater. Chem. Phys.* **2010**, *124*, 192–195. [[CrossRef](#)]
27. Gao, L.N.; Zhai, J.W.; Song, S.N.; Yao, X. The In-Plane Dielectric and Microwave Properties of Barium Stannate Titanate Thin Films. *Ferroelectrics* **2009**, *388*, 60–66. [[CrossRef](#)]
28. Jiwei, Z.; Bo, S.; Xi, Y.; Liangying, Z. Dielectric and ferroelectric properties of Ba (Sn_{0.15}Ti_{0.85})O₃ thin films grown by a sol–gel process. *Mater. Res. Bull.* **2004**, *39*, 1599–1606. [[CrossRef](#)]
29. Huang, H.H.; Wang, M.C.; Chen, C.Y.; Wu, N.C.; Lin, H.J. Effect of deposition parameters on the growth rate and dielectric properties of the Ba (Sn_xTi_{1-x})O₃ thin films prepared by radio frequency magnetron sputtering. *J. Eur. Ceram. Soc.* **2006**, *26*, 3211–3219. [[CrossRef](#)]
30. Kuo, Y.F.; Tseng, T.Y. Ba (Ti_{0.8}Sn_{0.2})O₃ Thin Films Prepared by Radio-Frequency Magnetron Sputtering for Dynamic Random Access Memory Applications. *Electrochem. Solid State Lett.* **1999**, *2*, 236. [[CrossRef](#)]
31. Song, S.N.; Zhai, J.W.; Yao, X. Substrate effect on in-plane dielectric and microwave properties of Ba(Sn_{0.15}Ti_{0.85})O₃ thin films. *Mater. Res. Bull.* **2008**, *43*, 2374–2379. [[CrossRef](#)]
32. Song, S.N.; Zhai, J.W.; Gao, L.N.; Yao, X.; Hung, T.F.; Xu, Z.K. Enhanced electric field tunable dielectric properties of Ba(Sn_{0.15}Ti_{0.85})O₃ thin films. *J. Appl. Phys.* **2008**, *104*, 096107. [[CrossRef](#)]
33. Halder, S.; Victor, P.; Laha, A.; Bhattacharya, S.; Krupanidhi, S.B.; Agarwal, G.; Singh, A.K. Pulsed excimer laser ablation growth and characterization of Ba (Sn_{0.1}Ti_{0.9})O₃ thin films. *Solid State Commun.* **2002**, *121*, 329–332. [[CrossRef](#)]
34. Tumarkin, A.V.; Zlygostov, M.V.; Gagarin, A.G.; Altyannikov, A.G.; Sapego, E.N. Planar Capacitive Structures Based on Ferroelectric Barium Titanate–Stannate Films on Sapphire for Microwave Applications. *Tech. Phys. Lett.* **2019**, *45*, 639–642. [[CrossRef](#)]
35. Tumarkin, A.V.; Stozharov, V.M.; Altyannikov, A.G.; Gagarin, A.G.; Razumov, S.V.; Kaptelov, E.Y.; Kozyrev, A.B. High tunable BaSn_xTi_{1-x}O₃ thin films for microwave applications. *Integr. Ferroelectr.* **2016**, *173*, 140–146. [[CrossRef](#)]
36. Song, S.; Gao, L.; Zhai, J.; Yao, X.; Cheng, Z. Crystal orientation dependence of the in-plane dielectric properties for Ba(Sn_{0.15}Ti_{0.85})O₃ thin films. *Appl. Surf. Sci.* **2008**, *254*, 5120–5123. [[CrossRef](#)]
37. Kozyrev, A.B.; Keis, V.N.; Koepf, G.; Yandrofski, R.; Soldatenkov, O.I.; Dudin, K.A.; Dovgan, D.P. Procedure of microwave investigations of ferroelectric films and tunable microwave devices based on ferroelectric films. *Microelectron. Eng.* **1995**, *29*, 257–260. [[CrossRef](#)]
38. Tumarkin, A.V.; Razumov, S.V.; Gagarin, A.G.; Altyannikov, A.G.; Stozharov, V.M.; Kaptelov, E.Y.; Pronin, I.P. The structure and dielectric properties of thin barium zirconate titanate films obtained by RF magnetron sputtering. *Tech. Phys. Lett.* **2016**, *42*, 143–145. [[CrossRef](#)]
39. Shibuya, K.; Mi, S.; Jia, C.L.; Meuffels, P.; Dittmann, R. Sr₂TiO₄ layered perovskite thin films grown by pulsed laser deposition. *Appl. Phys. Lett.* **2008**, *92*, 241918. [[CrossRef](#)]
40. Lotnyk, A.; Senz, S.; Hesse, D. Thin-film solid-state reactions of solid BaCO₃ and BaO vapor with (110) rutile substrates. *Acta Mater.* **2007**, *55*, 2671–2681. [[CrossRef](#)]
41. Lotnyk, A.; Senz, S.; Hesse, D. Formation of BaTiO₃ thin films from (110) TiO₂ rutile single crystals and BaCO₃ by solid state reactions. *Solid State Ion.* **2006**, *177*, 429–436. [[CrossRef](#)]
42. Tumarkin, A.V.; Al'myashev, V.I.; Razumov, S.V.; Gaidukov, M.M.; Gagarin, A.G.; Altyannikov, A.G.; Kozyrev, A.B. Structural properties of barium strontium titanate films grown under different technological conditions. *Phys. Solid State* **2015**, *57*, 553–557. [[CrossRef](#)]